Scientific Research Publishing

Atmospheric and Climate Sciences, 2026, 16(1), 83-105
https://www.scirp.org/journal/acs
ISSN Online: 2160-0422
ISSN Print: 2160-0414

Optical and Microphysical Characterization of Atmospheric Aerosols in Chad Based on Satellite Observations

Beuteube Rianbe Francois[1,2*], Galmai Orozi[1,2], Koumaguei Tchiroue[1,2], Ali Ahmat Younous[3], Mamadou Simina Drame[3], Fia Oung Zetna[1*]

[1]Department of Physics, Faculty of Exact and Applied Sciences, University of N'Djamena, N'Djamena, Chad
[2]Laboratory of Atmospheric, Climate and Environmental Physics (LAPACE), N'Djamena, Chad
[3]Simeon-Fongang Laboratory of Atmospheric and Ocean Physics, Cheick Anta Diop University, Dakar, Senegal
Email: *beuteube2012@gmail.com, *fiaoungzetna@gmail.com

How to cite this paper: Francois, B.R., Orozi, G., Tchiroue, K., Younous, A.A., Drame, M.S. and Zetna, F.O. (2026) Optical and Microphysical Characterization of Atmospheric Aerosols in Chad Based on Satellite Observations. *Atmospheric and Climate Sciences*, **16**, 83-105.
https://doi.org/10.4236/acs.2026.161006

Received: November 3, 2025
Accepted: December 15, 2025
Published: December 18, 2025

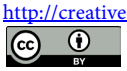

Abstract

This study evaluates the optical and microphysical properties of atmospheric aerosols over Chad using satellite data from the MODIS, MISR, SeaWIFS, and OMI sensors, as well as the MERRA-2 reanalysis, with the aim of identifying the most suitable instrument for their monitoring. A comparison of aerosol optical depth (AOD) values reveals a systematic underestimation by MERRA-2, while MODIS, MISR, SeaWIFS, and OMI tend to overestimate them. Linear correlation analysis shows that MODIS exhibits the strongest correlation with MERRA-2 (R = 0.62), followed by MISR (R = 0.61), SeaWIFS (R = 0.55), and OMI (R = 0.41). The spatio-temporal analysis of monthly variations reveals a high aerosol load during spring and summer, as confirmed by the annual cycles of AOD at 550 nm and the Ångström exponent (412 - 470 nm), indicating the predominance of desert dust. Conversely, the concentrations of other aerosol types remain low during both summer and winter. The aerosol index (AI), measured by OMI and TOMS, also highlights a strong presence of absorbing aerosols, with a maximum observed in May and respective minima in September and November. Analysis of the seasonal variability in the distribution of the Ångström exponent (AE) as a function of AOD shows the predominance of accumulation and coarse modes, mainly associated with mineral dust. These results confirm the reliability of the MODIS sensor for aerosol monitoring over Chad, where accumulation and coarse modes dominate the atmosphere.

Keywords

Aerosols, Airborne Sensors, MERRA-2, Optical and Microphysical Properties

1. Introduction

Chad, a sub-Saharan country located in the heart of Africa, shares borders with Libya to the north, Sudan to the east, the Central African Republic to the south, and Cameroon, Nigeria, and Niger to the west [1]. This strategic position results in significant climatic diversity, ranging from tropical and Sahelian zones to the arid desert regions of the Sahara. The Sahara Desert and its surrounding margins represent the most extensive and persistent sources of dust in the world. Annual dust emissions from the Sahara are estimated to range between 130 and 1600 megatons per year [2]. Several analyses based on satellite and ground observations have identified the foothills of the Ahaggar (in Mali) and Tibesti Mountains, as well as the Bodélé Depression in Chad, as the principal sources of Saharan dust [3]. Among these, the Bodélé Depression is recognized as the largest dust source in the world [4]-[6].

Chad's climatic diversity is also reflected in wind patterns that vary across regions [1]. The country is highly exposed to Saharan dust, as well as to anthropogenic emissions from transportation, domestic activities, and agriculture [7]. This paper deals with the characterization of aerosols in the Sahelian zone, particularly in Burkina Faso, based on MODIS observations and *in situ* measurements of the AERONET network on the Ouagadougou site (12.2˚N, 1.4˚W). Thus, a seasonal spatial distribution of aerosols made over the period from 2001 to 2016 gives a great variability of aerosols in Burkina Faso, whose maxima are encountered in spring, characterized by winds from the North East. This seasonality of aerosols is also shown by the annual cycles of optical, radiative, and microphysical parameters measured by AERONET between 1999 and 2006. Moreover, an analysis of these parameters shows the prevalence of mineral dusts characterized by low values of the Ångström coefficient α (440 - 870 nm < 0.5) associated with the maxima of AOT with high intensity in March. These dusts are confirmed by their scattering nature (SSA > 0.9) and the cooling noticed in the bottom of the atmosphere (BOA) and at the top of the atmosphere (TOA). Also, the climatology of the volume size distribution of aerosols shows a very great variability of particles in terms of size influenced by the thin and coarse pattern, where most sizes are between 1 and 10 μm. Desert dust is classified as one of the main types of atmospheric aerosols. The size of atmospheric aerosol particles ranges from 0.01 μm to 100 μm [8] [9], allowing them to remain suspended in the atmosphere for several hours before settling either through gravitational processes (dry deposition) or via scavenging by precipitation (wet deposition).

On a global scale, four main categories of aerosols can be identified, each with distinct physical, chemical, optical, and radiative properties: aerosols from biomass burning, aerosols from industrial and urban pollution, desert dust, and marine aerosols [10]. These aerosols contribute to climate change by modifying the composition and radiative behavior of the Earth's atmosphere, similar to greenhouse gases (GHGs) [11] [12]. They influence the planet's climate by altering both the incoming solar radiation and the outgoing terrestrial infrared radiation [13], a

process that affects the Earth's overall energy, or radiative, balance. According to [14], this balance varies depending on climatic zones (latitude, longitude, and altitude) and atmospheric components such as rainfall, aerosols, and precipitable water.

Since the beginning of the pre-industrial period (1850-1900), anthropogenic aerosols have made a significant contribution to global climate change [11]. The human impact on the climate during this period far exceeds that resulting from natural processes such as solar variability and volcanic eruptions. Changes in atmospheric composition due to variations in the properties of greenhouse gases (GHGs) and aerosols can lead to either warming or cooling of the global climate system, which encompasses the atmosphere, hydrosphere, land surfaces, and biosphere [12]. Due to their high spatial and temporal variability, detecting and characterizing atmospheric aerosols remains a significant challenge [10]. However, substantial efforts have been made to improve aerosol characterization through *in situ* atmospheric measurements and continuous satellite observations, such as those provided by MODIS and CALIPSO. Complementary data from ground-based networks like AERONET and from international field campaigns such as AMMA (2001 and 2006) have also been instrumental [15]. These characterization efforts have generally focused on studying the African monsoon and assessing its climatic, environmental, and socio-economic impacts.

Aerosols in the Chadian atmosphere are spread by the Harmattan (dry season), a northeast wind [16], and also by the monsoon, a southwest wind coming from the Gulf of Guinea (rainy season). In addition to these two main winds, there are the northeast trade winds and the winds carrying dust from Bodélé to the Atlantic and the Amazon, known as the Low Level Jet [17], which blow throughout the dry season and especially during spring.

Recent studies on atmospheric aerosols in Africa have highlighted the optical properties and size distribution of these particles [10] analyzed aerosol parameters at two AERONET stations in Mali, revealing a predominance of mineral dust with variable Ångström exponents and optical thicknesses [18] focused on urban aerosols in Ouagadougou, assessing their radiative forcing and reporting significant seasonal variations in optical properties, with extreme values observed during both the dry and wet seasons [19] conducted a multi-year analysis in Nigeria, identifying a mixed aerosol load dominated by the coarse mode, particularly during the dry season, and noted variations in the Ångström exponent and single scattering albedo [20] emphasized the importance of infrared remote sensing for aerosol characterization, highlighting its potential to improve understanding of their climatic impacts. Finally, [21] confirmed the dominance of mineral dust through a spatio-temporal analysis of its optical and microphysical properties in Burkina Faso. Collectively, these studies underscore the complexity and variability of aerosol characteristics across Africa [10] [18]-[21].

The present study aims to characterize atmospheric aerosols in Chad through a spatio-temporal analysis of their optical and microphysical properties using the

MODIS, SeaWIFS, MISR, TOMS, and OMI satellite sensors and the MERRA-2 reanalysis, in order to assess the most suitable sensor for studying atmospheric aerosols in Chad.

2. Study Areas, Data, and Methods

2.1. Presentation and Description of the Study Areas

The climate of Chad varies from arid in the north to tropical in the south, with irregular rainy seasons (May to October) and a long dry season (November to April) [1] [14] [22]. Climate variations influence the dispersion and concentrations of aerosols [14]. The following cities were selected based on Chad's climate zones.

Table 1. Geographical coordinates for the study area.

Towns	Latitudes (Degrees)	Longitudes (Degrees)	Altitudes (m)
Bodélé	16.88˚N	18.55˚E	181
Salal	14.84651˚N	17.21864˚E	270
N'Djamena	12.1067˚N	15.0444˚E	298
Mongo	12.1828˚N	18.6847˚E	404
Pala	9.364166˚N	14.9044˚E	457
Goré	7.928886˚N	16.635025˚E	428

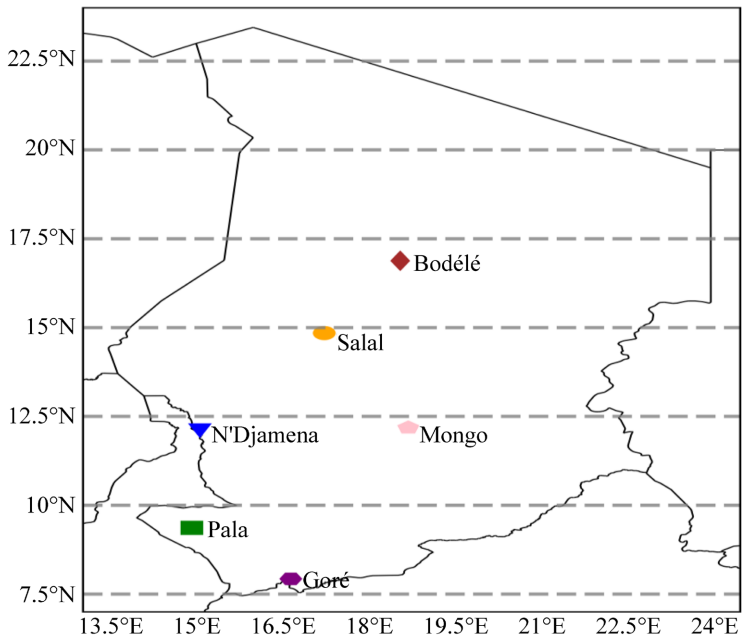

Figure 1. Study areas.

These cities are chosen according to climatic zones and are also represented in Figure 1, including isohyets, which provide more detail for their analysis, as well

as their geographical characteristics indicated in Table 1. Aerosol-carrying winds from different countries in the Sahara pass through the Sahel, such as the Harmattan, whose corridor is formed by the Tibesti-Ennedi-Lake Chad triangle [23]. It is predominant in winter (December to February) in Chad. It strongly influences the climate of the Sahel and some of the northern regions of Chad. The monsoon, on the other hand, is a system of periodic winds in tropical regions around the world [10]. Coming from the southwest, it brings rainfall and balances temperatures. It has a significant impact on the climate of the Sahel and southern Chad and promotes the development of agriculture and ecosystems [1].

2.2. Methods

2.2.1. Instrumentation

The instrumentation is based on a set of satellite sensors whose characteristics are summarized in Table 2. These sensors are used by some authors in their aerosol studies. Some of them are also referenced in Table 2.

Table 2. Sensors and their characteristics.

Sensors	Temporal Resolution	Wavelengths	Periods	References
SeaWiFS	Monthly	555 nm	1997-2010	[24] [25]
MODIS-TERRA	Monthly	550 nm	2000-2024	[7] [26]-[28]
MISR	Monthly	555 nm	2000-2017	[25] [29] [30]
OMI	Daily	500 nm	2004-2024	[30]-[33]
TOMS	Daily	U.V	1996-2005	[31] [34]
MERRA-2	Monthly	550 nm	1994-2024	[25]

2.2.2. Methodologies for Analysis and Validation of Observations

The validations concern monthly and interannual average data from satellite sensors with the following spatial resolutions: MODIS-Terra (1˚), SeaWIFS (1˚), MISR (0.5˚), OMI (1˚), TOMS (1.0 × 1.25˚), and MERRA-2 reanalysis (0.5 × 0.625˚), measured at wavelengths of 500 nm, 550 nm, and 555 nm. The optical thickness, Ångström exponent, aerosol index, and main types of aerosols were studied in Chad. We analyzed the data using Python. The data were collected in the reflective range [0.4; 2.5 μm], and preferably in the visible and near-infrared range [0.4; 1.0 μm], where aerosols have the strongest optical impact. The choice of MERRA-2 as a reference for the study of the intercomparison of AOD is justified by the fact that it integrates observations from various satellites, thus providing a coherent and homogeneous dataset over an extended period. Furthermore, it uses a general circulation model that simulates atmospheric processes and the interactions between aerosols and climate, allowing for a better estimation of AOD.

2.2.3. Optical Properties of Atmospheric Aerosols

The optical thickness of an aerosol (AOD for aerosol optical depth or AOT for aerosol optical thickness) is a dimensionless quantity that characterizes the transparency of the atmosphere to solar radiation [35]. It corresponds to the amount of light that is absorbed or scattered when light passes through a medium, such as a layer of the atmosphere, a cloud, or any other transparent or translucent material [36]. It is a fundamental and macroscopic parameter that is most commonly used in the characterization of atmospheric aerosols [9]. AOD is determined according to the filters of the available detectors and according to the devices, as there may be more or fewer wavelengths depending on the sensors. However, for a sensor such as the AERONET photometer, there are always at least four: 440, 675, 870, and 1020 nm. Using direct solar irradiance measurements from the ground, the aerosol optical depth (AOD) is calculated using Beer-Lambert's law (1852), solved for atmospheric boundary conditions:

$$I_\lambda = I_{\lambda,0} exp\left[\left(-m\,AOD\right)\right] R^2 \tag{1}$$

where I_λ is the irradiance measured at ground level; $I_{\lambda,0}$, extraterrestrial irradiance at wavelength λ; m is the optical air mass along the line of sight connecting the observation point and the sun; R, is the distance between the Sun and Earth in astronomical units, normalized to variations around the average distance[35] [37]. The optical thickness is extracted by eliminating all other extinguishers, including traces of gas and physical processes such as Rayleigh scattering [36]. All these assumptions together allow us to deduce that:

$$\frac{I_\lambda}{I_{\lambda,0}} = exp\left(-AOD\right) \quad \text{so} \quad AOD = -\ln\left(\frac{I_\lambda}{I_{\lambda,0}}\right) \tag{2}$$

A high optical thickness value of one or more indicates a sky heavily laden with aerosols (or clouds, if it is not possible to distinguish between the optical thickness of aerosols and that of clouds) and therefore not very transparent, while a low optical thickness indicates a clearer sky. For this reason, optical thickness is particularly important near source regions [38]. The spectral dependence of optical thickness provides information on particle size via the Angström exponent [39]. They are linked by the Angström formula (1929):

$$\alpha = -\frac{d\ln AOD_\lambda}{d\ln\lambda} = -\frac{\ln\left(\frac{AOD_{\lambda 1}}{AOD_{\lambda 2}}\right)}{\ln\left(\frac{\lambda_1}{\lambda_2}\right)} \tag{3}$$

where $AOD_{\lambda 1}$ and $AOD_{\lambda 2}$ are optical thicknesses at respective wavelengths λ_1 and λ_2. α varies very slowly with wavelength, both in the visible and infrared ranges. It is unique in a spectral band [40]. In general, if:

- $\alpha < 1 \rightarrow$ presence of coarse particles (desert dust, sea salt);
- $\alpha \approx 1 \rightarrow$ mixture of particles of various sizes;
- $\alpha > 1 \rightarrow$ presence of fine particles (urban pollution, smoke, anthropogenic

aerosols).

In practical terms, these two parameters are linked by the empirical formula [21] [29]:

$$AOD_{\lambda 1} = AOD_{\lambda 1}\left(\frac{\lambda_1}{\lambda_2}\right)^{-\alpha} \tag{4}$$

Optical thickness and the Ångström exponent are considered key parameters in the study of aerosol climatology [10].

In Equation (4), α, $AOD_{\lambda 1}$ and $AOD_{\lambda 2}$ are defined at wavelengths λ_1 and λ_2. Subsequently, a linear regression analysis is performed based on Equation (5), where l is the slope of the line and B is the point of intersection between the line and the y-axis[25] [29].

$$AOD_{satellite} = l \times AOD_{MERRA-2} + B \tag{5}$$

The quantities (l, B) and the correlation coefficient R of the intercomparison serve as an indication of the local and spatial characteristics of AOD over time [41]. The slope l of the linear regression equation (5) reveals the extent to which the assumed aerosol model represents that of the observed area, while B relates the error caused by surface reflection [42] [43]. Thus, the regression equation provides information on the factors affecting the correlation [44] and, in the case of a good correlation, B must be zero and l must tend towards unity [42].

The parameter that distinguishes absorbing aerosols from non-absorbing aerosols in the ultraviolet and visible ranges (e.g., desert dust aerosols, smoke aerosols, and volcanic ash) is the aerosol index (AI) [35]. This is a qualitative, unitless measure that expresses relative intensity. Absorbing aerosols can be characterized by the AI, which emphasizes the optical properties, concentration, and altitude of the aerosol. It is used to detect and monitor aerosol plumes on a global scale. It is based on spectral differences between light scattered and absorbed in the atmosphere:

$$AI = -100 log_{10}\left(\frac{I_{mesured}(\lambda_2)}{I_{calculed}(\lambda_1)}\right) \tag{6}$$

where $I_{mesured}(\lambda_2)$ is the measured intensity of backscattered light at a wavelength λ_2 by a satellite sensor and $I_{calculed}(\lambda_1)$ is the calculated intensity of backscattered light at a wavelength λ_1 in pure Rayleigh atmosphere [35]. Wavelengths λ_1 and λ_2 are generally ultraviolet (for example, between 340 and 380 nm). In general, if:

- $AI > 0 \rightarrow$ presence of absorbing aerosols (desert dust, forest fire smoke, volcanic ash, etc.).
- $AI \approx 0 \rightarrow$ clear atmosphere or presence of non-absorbent aerosols.
- $AI < 0 \rightarrow$ possibility of error or specific atmospheric conditions (example of erroneous corrections).

3. Results and Discussions

3.1. Comparison between Monthly Averages of AODs

The analysis focuses on time series of monthly AOD averages from the MERRA-

2 reanalysis and MODIS, MISR, OMI, and SeaWiFS satellite sensors. Figure 2 shows that AOD values vary between 0.31 and 0.81 depending on the sensor, for different periods. The MERRA-2 AOD values (0.46 to 0.69) for N'Djamena are more accurate, indicating an underestimation compared to satellite observations. The monthly peaks for MODIS (0.73), SeaWiFS (0.81), OMI (0.74), and MERRA-2 (0.69) are recorded in March or April, while that of MISR (0.75) appears in May. These maxima correspond to the dry season (spring), which is the period when soil warming promotes the uplift of particles. A second peak is observed in October (autumn), reinforcing the idea that particle load is higher outside the rainy season. In the post-monsoon period and in winter, the thinner atmospheric boundary layer traps pollutants near the surface, increasing the AOD. The seasonal variability of AOD reflects changes in sources: Saharan dust, biomass combustion, and other anthropogenic emissions, with a clear contrast between the dry season (Harmattan) and the wet season (monsoon), which is not conducive to the suspension of atmospheric aerosols [45].

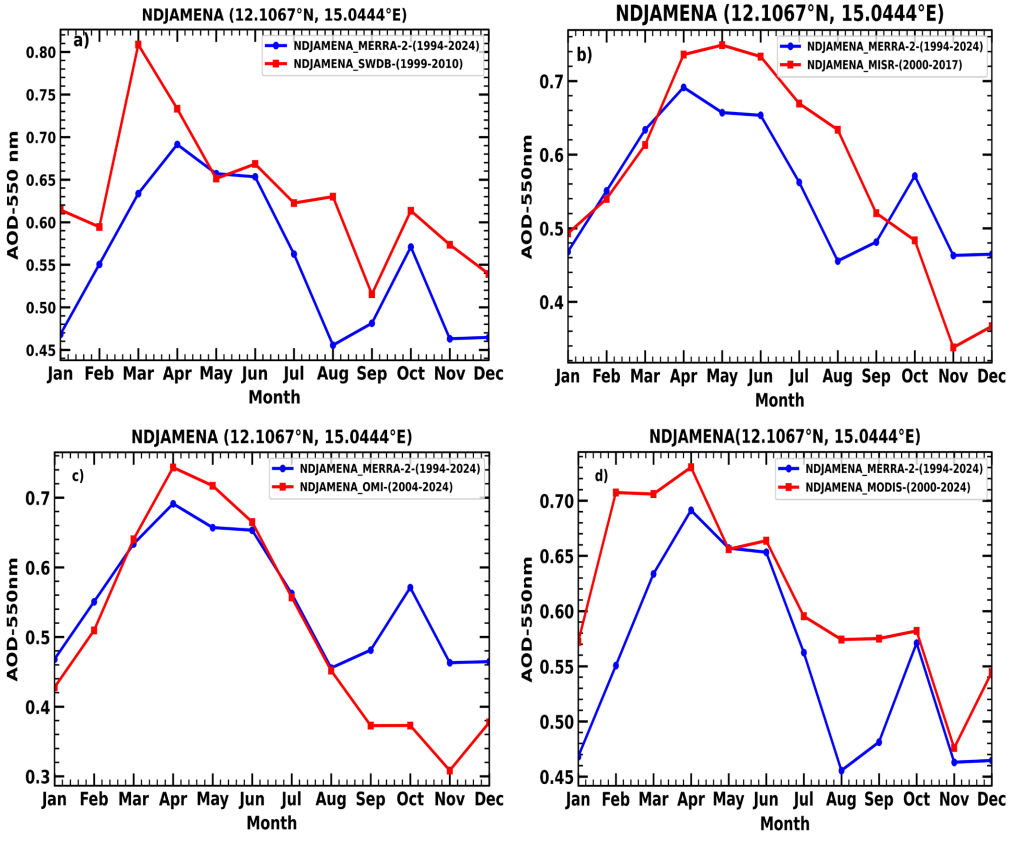

Figure 2. Time series of monthly AOD averages for N'Djamena.

3.2. Intercomparison of Satellite Sensors and MERRA-2 for N'Djamena

The linear regression analysis clearly shows the correlation between the AODs measured by SeaWiFS, MISR, OMI, and MODIS at 500 nm, 550 nm, and 555 nm,

respectively. This is illustrated in Figures 3(a)-(d). It indicates a good correlation between MODIS and MERRA-2 measurements with a linear regression coefficient R = 0.62 (Figure 3(d)). Unlike the other sensors, SeaWiFS (R = 0.55), MISR (R = 0.61), and OMI (R = 0.41) are the most representative satellite models for long-term aerosol characterization. The accuracy of airborne sensors is also evident in the slopes of the regression lines: 0.6314, 1.0275, 1.1129, and 0.4853 obtained respectively between SeaWiFS and MERRA-2 (Figure 3(a)), MISR and MERRA-2 (Figure 3(b)), OMI and MERRA-2 (Figure 3(c)), and MODIS and MERRA-2 (Figure 3(d)). However, the smallest intersection point is given by the intercomparison between MISR and MERRA, which is 0.0069. This shows that this sensor is more accurate than the others. However, there is a very large inconsistency in the OMI measurements. In addition to its relatively high correlation coefficient (R = 0.41) and slope (l = 1.113), its intercept constant is virtually zero (B = 0.0919). Thus, the OMI model shows a very large deviation from the MERRA-2 measurements, justifying the overestimation revealed by the time series of monthly AOD averages and the shift in the aerosol peak in spring, mostly in April.

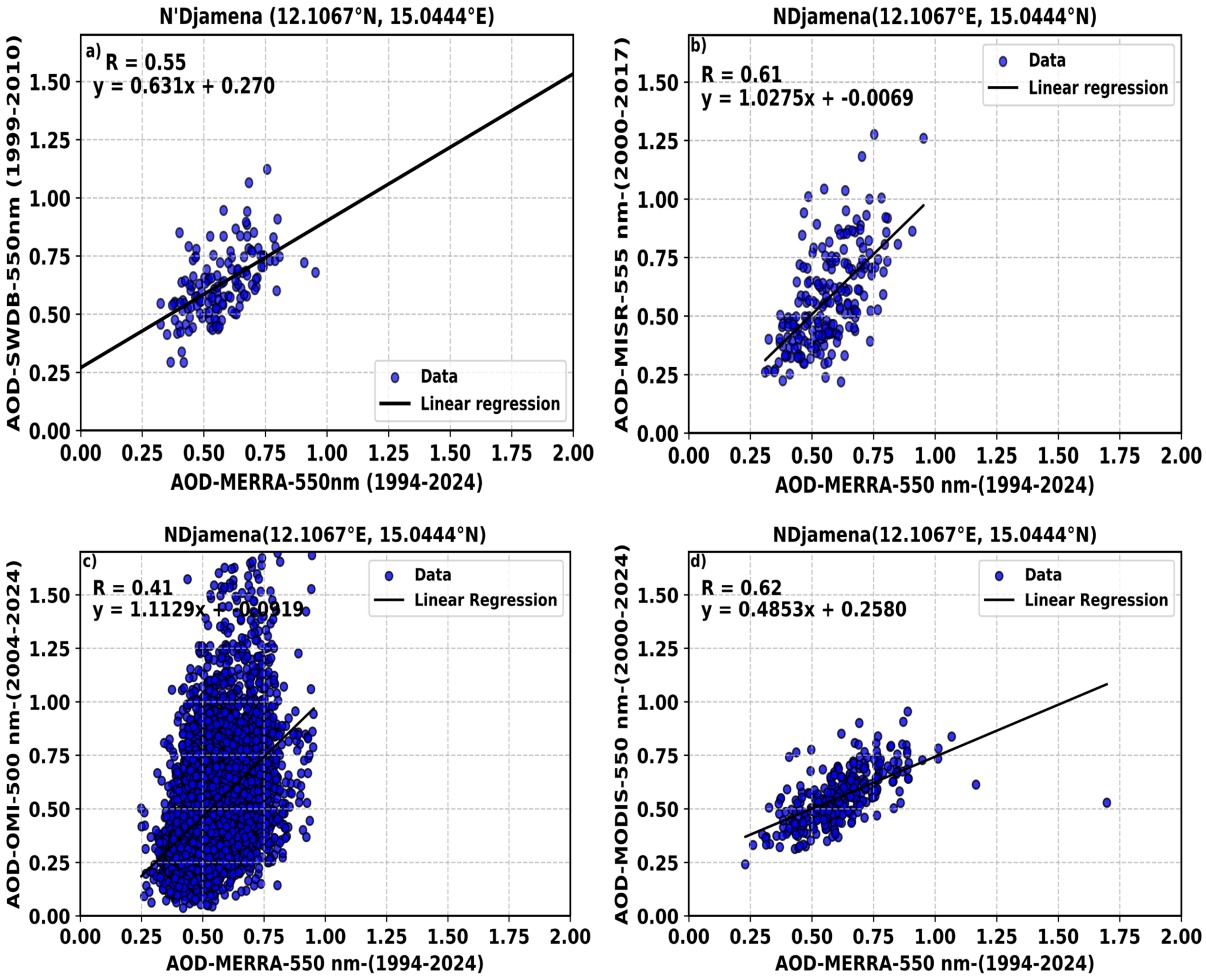

Figure 3. Linear regression curves illustrating the correlations of MODIS, MISR, SeaWIFS, IMO TOMS, and MERRA-2 data.

Each of these sensors uses different retrieval algorithms that may vary in their approach to estimating AOD, leading to different estimations, as the algorithms often rely on assumptions about the composition of aerosols and the properties of the surface, which, if incorrect, can result in errors. Additionally, these sensors often filter out data affected by clouds, which can lead to the underestimation of AOD in cloudy regions, as clouds can interfere with aerosol measurements, making it difficult to distinguish between the signals from aerosols and those from clouds. Consequently, they can lead to discrepancies in their AOD estimates.

3.3. Study of the Spatial Variability of Aerosols in Chad

3.3.1. Annual Cycles of Optical Thicknesses

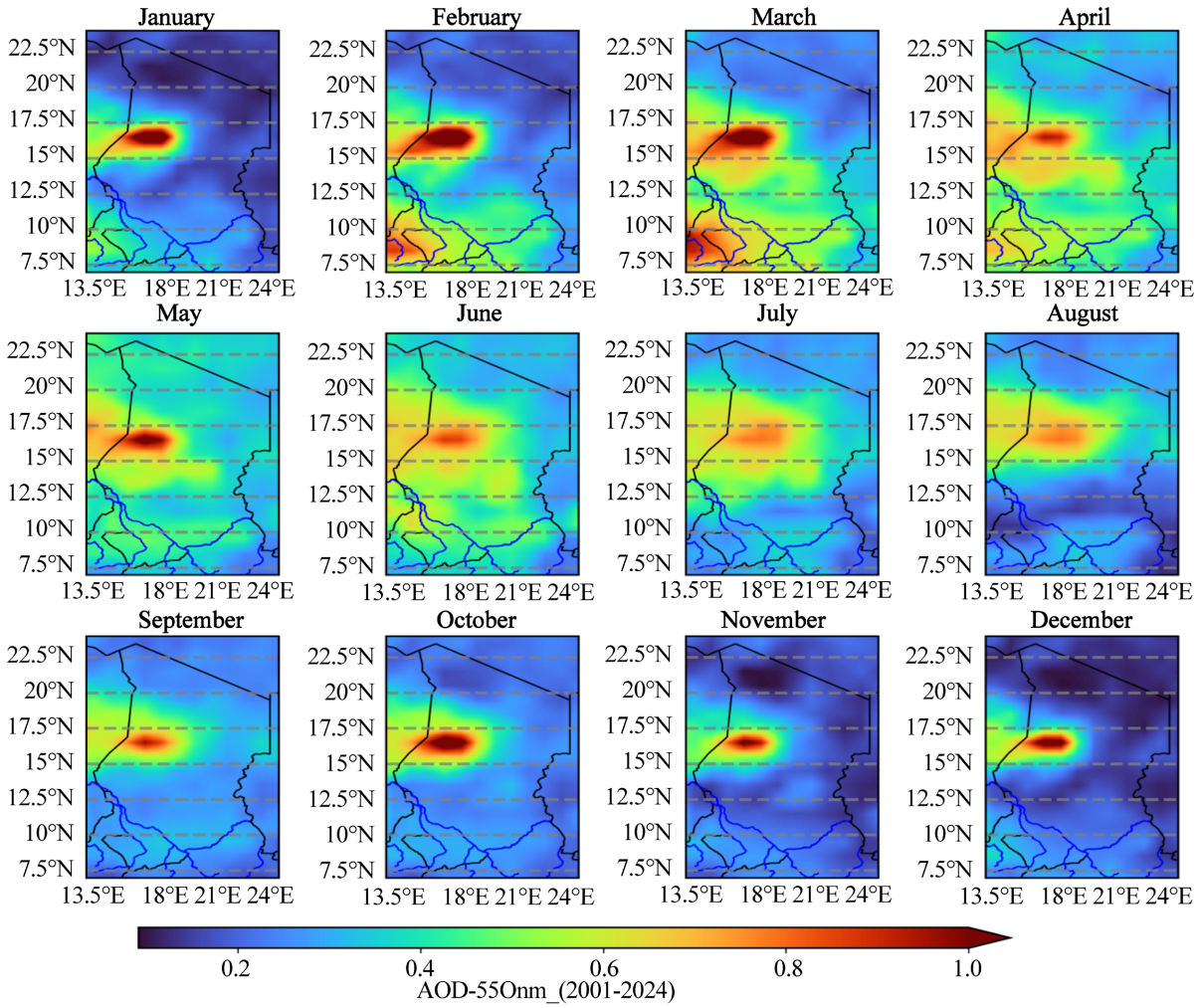

Figure 4. MODIS-TERRA monthly averages of AOD for the period: 2000-2024 in Chad.

Chad experiences significant spatial and temporal variability in dust emissions. Figure 4 shows an interannual and monthly climatology of AOD, with a maximum observed in winter (December to March), mainly in the northeast (17˚N - 18˚E), under the influence of the Bodélé epression, the world's main source of desert dust

[2] [16]. Between January and February, AOD peaks reflect intense transport of Saharan dust. In spring (April-May), AOD gradually decreases but remains high in the north, indicating persistent activity. In summer (June to September), AOD becomes moderate (0.4 - 0.5) and spreads across the entire country, due to the effect of convective systems and humidity, which limits dust uplift [39]. This period is also marked by emissions from bushfires and biomass combustion in the south. In autumn (October to November), an increase in AOD is observed, linked to the return of dry, arid winds that promote dust resuspension.

3.3.2. Spatial and Seasonal Distribution of Aerosol Shape

The Angström exponent helps identify the nature of aerosols: values below 1 indicate coarse particles (mineral dust), while values above 1 signal fine particles (such as pollutant particles). **Figure 5** reveals a coexistence of these two types throughout the year, with varied seasonal variations. In winter (DJF), coarse particles dominate in the north, reflecting the Saharan influence of mineral dust from Bodélé. In the south and southwest, fine particles thrive due to several causes, including lower temperatures and increased humidity that favor the formation and persistence of fine particles such as organic aerosols and sulfates. Human activities, like biomass combustion for heating or cooking, can also increase the concentration of fine particles in these regions. Additionally, precipitation can clean the atmosphere of larger particles, resulting in a higher concentration of fine particles during this season in Chad.

In spring (MAM), larger particles are concentrated in the north due to the prevailing influence of the Bodélé depression during this season, which is consistent with the AOD peaks observed in **Figure 3**. A low concentration of fine particles around Emi Koussi and in the southeast is linked to the influx of dust from predominant desert regions, which can dilute the presence of fine particles often associated with organic aerosols or combustion products from the Gulf of Guinea. In summer (JJA), fine particles are located in the north, center, and east of Chad. They are brought in by the northeastern wind (Harmattan) and the positioning of the monsoon (southwest). Summer is often characterized by higher temperatures and increased relative humidity, favoring the formation of fine aerosols, such as organic aerosols and sulfates. Coarser particles are more present in the south and around Bodélé, coming from strong winds lifting dry sediments and spreading combustion residues northward. In autumn (SON), both the south and north experience a diversity of aerosols linked to the transition between the monsoon and the Harmattan, marked by the movement of the intertropical convergence zone (ITCZ) [16] [38]. Hydric erosion followed by rapid drying also promotes sediment mobilization. The low AE values observed in **Figure 5** in the north of Chad are closely related to the nature of mineral dust transported from the Bodélé depression, corresponding to larger particles that affect the light diffusion less in the observed wavelengths. This highlights the predominant role of mineral dust in the optical characteristics of aerosols in this region.

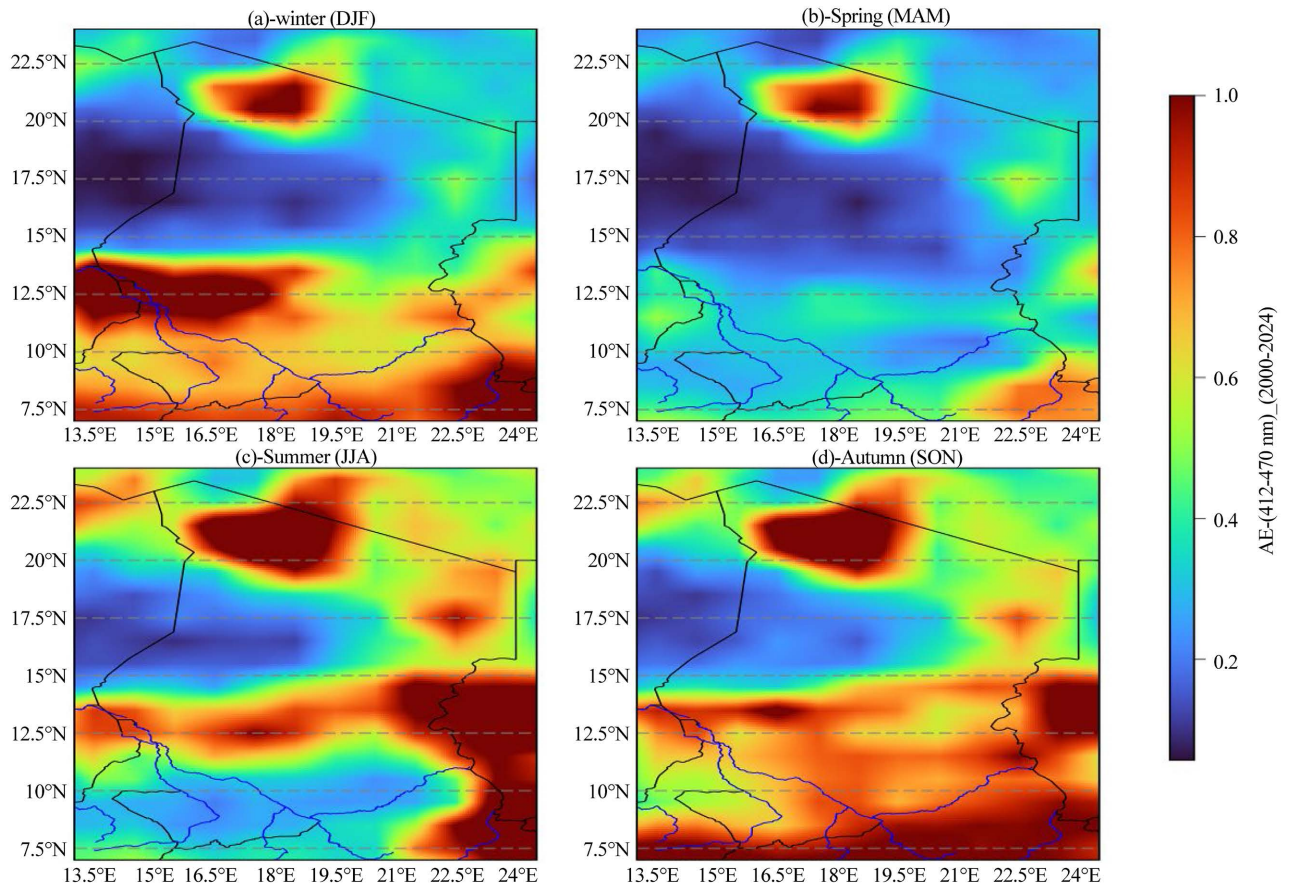

Figure 5. Spatial and seasonal distribution of Angström exponent by MODIS-TERRA for the period: 2000-2024 in Chad.

3.4. Combined Analysis between MERRA-2 and MODIS

Figure 6 shows the time series of interannual and monthly AOD averages obtained by MODIS-Terra inverted between 2000 and 2024 for Chad in general and for N'Djamena in particular. These time series are compared with those produced by the MERRA-2 reanalysis of N'Djamena. MERRA-2 (blue curve) shows the maximum aerosol concentration in spring, clearly highlighted by the AOD peaks in April. The same is true for MODIS (red curve), which is in good agreement with the AOD maxima, also in spring (April). However, in addition to spring, MODIS reproduces the AOD peak in summer (June). This evolution of atmospheric particles is corroborated by the seasonality of aerosols, as illustrated in **Figure 5** and **Figure 6**. Aerosols can be distributed vertically and horizontally. Studies conducted by [15] [24] show that the vertical distribution of aerosols allows the aerosol layer to be located in summer between 3 and 6 km in West Africa. Thus, the presence of particles in the upper troposphere could well explain the observation of the summer AOD peak at MODIS, which has a much wider field of view than MERRA-2, whose data-providing device may be limited by precipitation and cloud cover. The particles observed in summer are mainly mineral dust from the long-range transport of aerosols contained in the Saharan air layer, and also due to convective systems. On the other hand, the AOD minima in August (blue curve), November (red curve),

and December (green curve) are probably due to the elimination of particles by sedimentation, following water recovery or atmospheric leaching due to heavy precipitation. However, the maximum aerosol levels observed in Chad from October to December are probably linked to the transition between the monsoon and the Harmattan, which is very turbulent during this period [15].

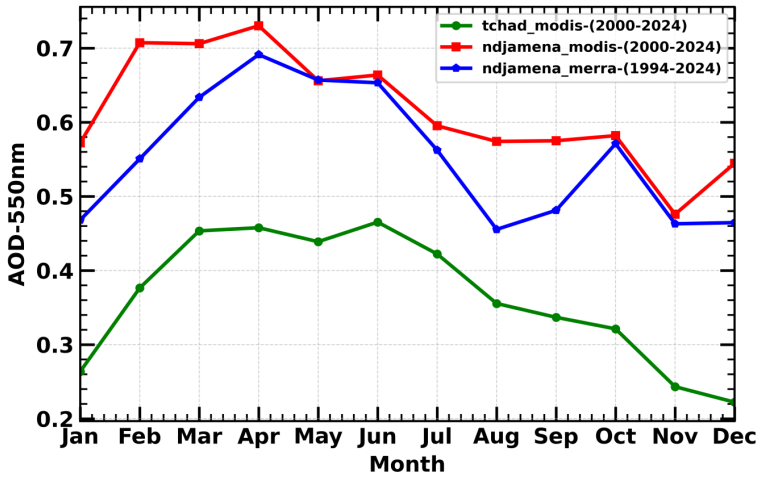

Figure 6. Representation of the annual AOD cycle for Chad (green) and for N'Djamena observed by MERRA-2 (blue) and MODIS (red).

3.5. Optical Analysis of Aerosols according to Climate Zones

Figure 7(a) illustrates the monthly averages of aerosol optical depth (AOD) at 550 nm for several cities in Chad. Maximum concentrations occur in summer, particularly in August, except in Pala and N'Djamena, where peaks occur in spring (April). This difference can be explained by the persistence of the Harmattan, which is active from winter to spring, before the transition to the monsoon. This dynamic reflects the spatial and temporal variability of aerosols in Africa. The maximum AOD values in Mongo (0.47) and Salal (0.53) can be explained by the combined influence of the monsoon and the Harmattan, which transports Saharan dust [21] [7]. In N'Djamena (0.62), Pala (0.52), and Goré (0.50), high AOD values are linked to both Bodélé dust (0.47) and biomass burning in the Gulf of Guinea (October to May). Local emissions from human activities and long-range transport contribute to elevated AOD levels in large urban areas such as N'Djamena (AOD = 0.62), Ouagadougou (AOD = 0.64) [21], and Banizoumbou (AOD = 0.62) [30]. **Figure 7(b)** highlights the predominance of aerosols in spring and summer, while the Angström exponent maxima occur in autumn (September) and winter (December), and the minima occur in summer (June), in connection with the action of the monsoon, which stirs up sediments. In August, fine desert particles dominate due to long-range transport. In autumn, peaks in the Angström exponent at Pala and Goré reflect the impact of aerosols from the transition between the monsoon and the Harmattan, characterized by intense convective systems and easterly winds that generate local dust emissions.

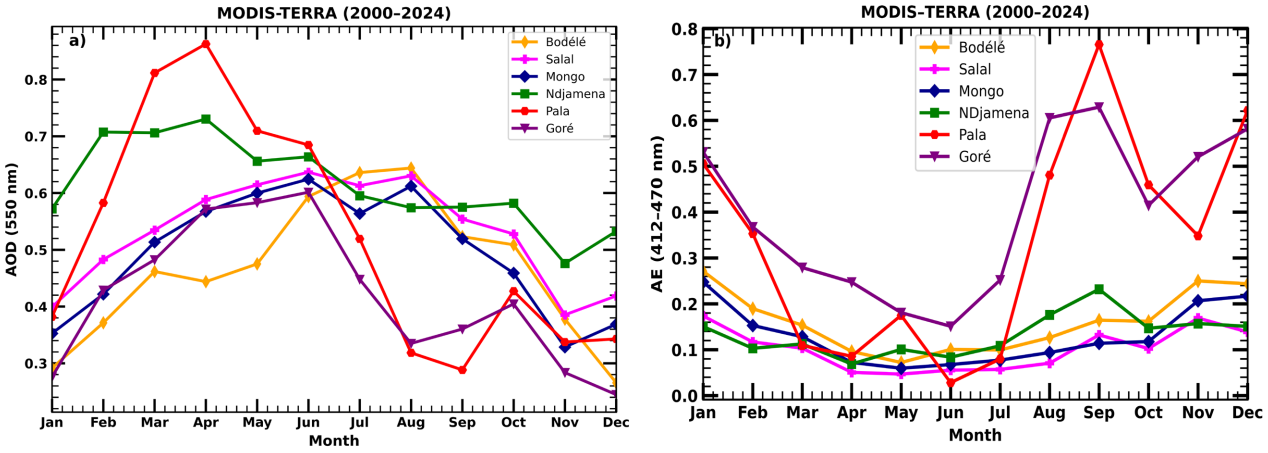

Figure 7. Interannual monthly averages of optical depth (AOD) (a) and Angström exponent (AE); (b) were observed at Bodélé (orange), Salal (pink), Mongo (dark blue), N'Djamena (green), Pala (red), and Goré (purple).

3.6. Aerosol Index in N'Djamena

To analyze the influence of large-scale meteorological factors on the mobilization of absorbing aerosols, two satellite datasets were examined: OMI (2004-2024) and TOMS-EP (1996-2005), as shown in **Figure 8**. These sensors measure the aerosol index (AI), an indicator of the presence of absorbing aerosols in the atmosphere. TOMS-AI evaluates the difference in ultraviolet backscattering between an atmosphere containing aerosols and a pure Rayleigh atmosphere [16], allowing the distinction between absorbing aerosols, such as soot (positive AI), and non-absorbing aerosols, such as sulfates (negative AI) [46]. An AI value of zero indicates the absence of aerosols in the atmosphere. Both OMI-AI and TOMS-AI are used to detect large dust plumes from deserts, such as those crossing the Sahel, or smoke emissions from forest and bush fires. The OMI-AI and TOMS-AI indices reach their respective peaks in May (1.2 and 2.4). Chad records particularly high concentrations of absorbing aerosols in spring (March to May), resulting from the superposition of several natural and anthropogenic sources. Among the natural sources, the Bodélé depression, located in northeastern Chad, is one of the world's main sources of desert dust emissions [17] [31]. During this period, easterly and northeasterly winds (the Harmattan) reach maximum intensity and transport large quantities of mineral particles rich in iron oxides, which are highly absorbing in the visible and infrared ranges [47].

At the same time, the dry season at the end of winter and during spring corresponds to an intensification of bush and savanna fires in the Sahelian and Sudanian zones. These biomass fires release significant amounts of black carbon (soot) and organic carbon, whose optical properties enhance the radiative absorption of aerosols [48] [49].

Finally, local urban sources, particularly domestic wood and charcoal burning as well as road traffic, contribute significantly to the atmospheric load of absorbing aerosols [50]. Spring weather conditions, characterized by high temperatures and a shallow atmospheric boundary layer, limit vertical dispersion and promote the

accumulation of particles over the Chadian atmosphere. The minimum AI values, observed in September (0.5) and November (1.1), are caused by factors such as rain washout, reduced dust emissions due to wet soils and vegetation, changes in air trajectories (supply of cleaner or moister air), and optical effects related to humidity (increased scattering, relative decrease in absorption).

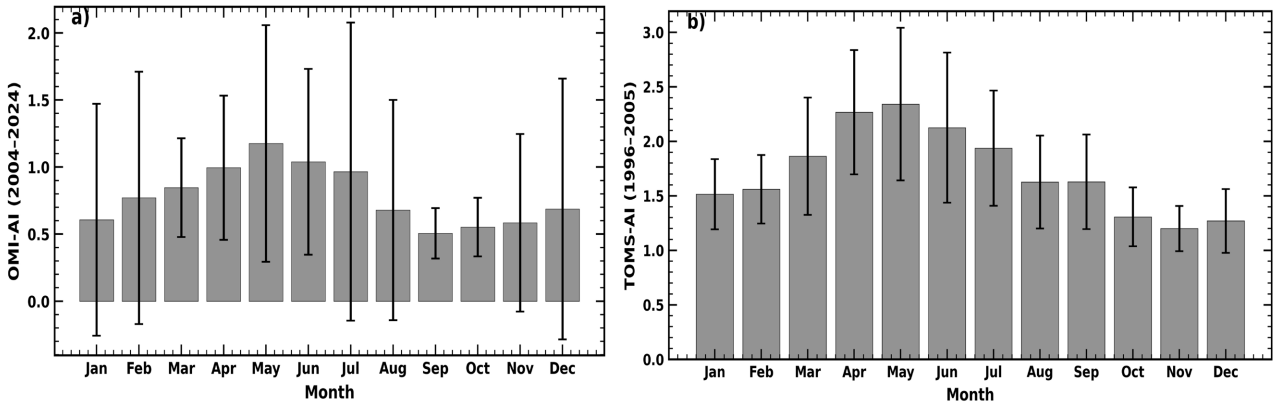

Figure 8. Variability of monthly averages of OMI-AI and TOMS-AI in Chad for the periods 2004-2024 and 1996-2005.

3.6.1. Seasonal Distribution of AE based on AOD

Determining the type of aerosols essentially requires knowledge of their optical and physical properties, which depend on both wavelength and solar and terrestrial radiation. The combined use of the descriptive properties of aerosol load or optical depth (AOD) and Angström exponent (AE) is the most widespread and widely used technique for classifying various types of aerosols [35].

Figure 9 shows the seasonal variations in AE as a function of AOD in N'Djamena. For all seasons, the highest values of the monthly averages of the Angström exponent correspond to low values of optical depth. The monthly average data are from MODIS-TERRA. These two parameters provide information on the presence and class of aerosols (coarse mode, accumulation mode, and fine mode). AE values are specific to particle types: AE ≈ 0 for large particles such as desert dust and AE > 1 for fine particles such as those produced by biomass combustion or industrial pollution.

The contribution of accumulation-mode aerosols is particularly significant in summer, fall, and spring, suggesting their predominance in this region during these seasons. The substantial presence of accumulation-mode particles in the atmospheric column above a location is associated with anthropogenic sources, including biomass burning, transportation, and agricultural activities, as well as the presence of the fine mode, which is slightly observed in spring and winter [11]. Throughout all seasons, the atmospheric aerosol content consists of a mixture of both accumulation and coarse modes. Accumulation-mode aerosols are especially dominant in N'Djamena, followed by coarse-mode aerosols. This finding is consistent with the study on lithometeors in N'Djamena conducted by [51]. The predominance of these modes can be explained by the city's geographical location

and locally generated wind patterns, which transport particles from the Sahara Desert.

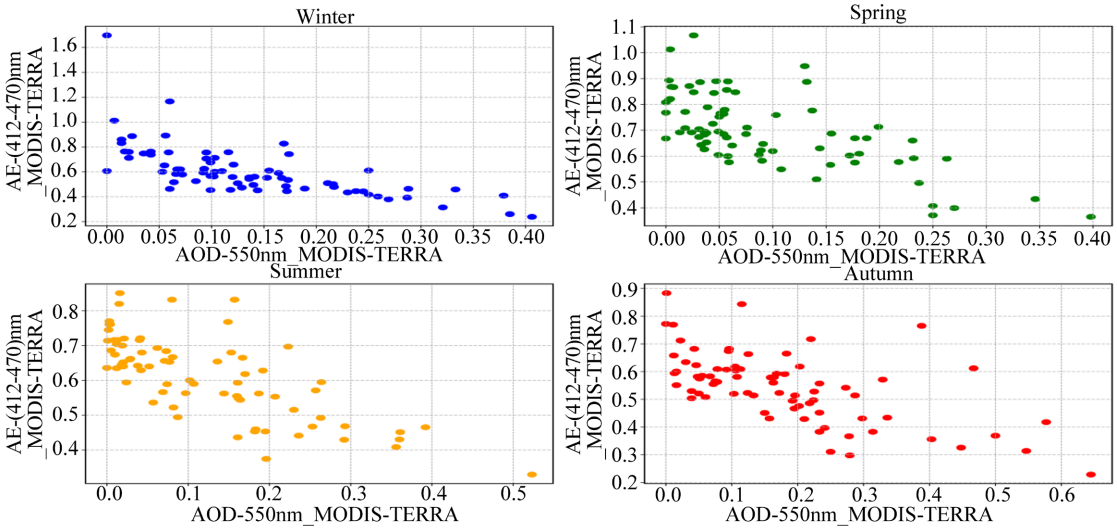

Figure 9. Seasonal distribution of AE based on AOD in N'Djamena for the period 2000-2024.

3.6.2. Classification of the Main Types of Atmospheric Aerosols in N'Djamena

The main objective is to analyze and evaluate the percentage of atmospheric aerosol types and to identify the most predominant type of aerosol during all seasons in N'Djamena. We followed the methodology as in the study by Ali M. Al-Shalihi (2018), which focused on the characterization of aerosol types based on their optical properties in the city of Baghdad, Iraq. Unlike that study, this classification was based on the concentrations of different aerosol types. To this end, we analyzed the concentrations of these main types of atmospheric aerosols derived from MERRA-2, using the site: https://giovanni.gsfc.nasa.gov/giovanni/. This allowed us to obtain results in percentages, as these different types of aerosols have varying climatic impacts depending on their concentrations. For example, dust and sulfates can have a cooling effect by reflecting sunlight, while carbonaceous particles (like black carbon) tend to warm the atmosphere. Distinct modeling allows for the evaluation of specific contributions to climate feedback.

Figure 10 shows the percentage contributions of the main aerosol types over N'Djamena. The results indicate that desert dust is the dominant component in this region. It should be noted that aerosol types are influenced by synoptically variable sources, the strength of sinks, transport pathways, local meteorological conditions, and vertical mixing processes. In addition, particle growth mechanisms such as humidification and hygroscopic growth play an important role in modifying aerosol characteristics [52].

The aerosols affecting N'Djamena originate mainly from the Sahara and Sahel regions. Other sources include agricultural activities such as plowing, construction work, and unpaved roads. However, anthropogenic emissions from traffic, industry,

and transportation contribute significantly, especially in capital cities. For example, in Baghdad (Iraq), these activities account for about 38% of total emissions [35].

In winter, their contribution rises to 89.1%. Organic aerosols, originating from biomass combustion (wood for heating) and soil erosion, account for only 5.5%, while sulfate aerosols contribute 3.6%, mainly from volcanic eruptions in East Africa [13] and other regions. Additional minor sources include the oxidation of dimethyl sulfide (DMS), savanna fires, fossil fuel combustion, industrial emissions, agricultural activities, and urban pollution. Carbonaceous aerosols and sea salts, representing small fractions (1.7% and 0.3%, respectively), are primarily produced by agricultural burning (stubble and wood) and industrial processes, as well as by natural atmospheric mechanisms. Sea salts are also transported southward by the Harmattan, which carries dust and salts from the Sahara Desert (**Figure 10(a)**).

In spring, dust aerosols contribute more significantly (93.5%) than during other seasons. This increase results from a combination of climatic factors, such as strong winds during the dry season, including the Harmattan, and anthropogenic factors such as farming, slash-and-burn practices, overgrazing, and deforestation, which enhance soil erosion, particularly in uncultivated areas. These human activities, combined with drought conditions, release large amounts of particles into the atmosphere, which are subsequently transported by winds during this period. Sulfate aerosols, which make a smaller contribution (2.8%), originate from volcanic eruptions, bush fires, and the combustion of fossil fuels in vehicles and power plants, as well as from industrial emissions. Once emitted, these particles can undergo chemical transformations to form secondary sulfate aerosols. Organic aerosols, with a similar contribution (2.5%), are mainly of natural origin, produced by wind erosion of dry soils and biomass burning, including vegetation fires and agricultural combustion. Additional sources may include secondary organic aerosols formed through chemical reactions in the atmosphere. The relatively low contributions of carbonaceous aerosols (0.9%) and sea salts (0.3%) can be attributed to changes in wind patterns that limit their transport from sources such as desert sand and burned biomass to Chad, reduced biomass burning activity at the beginning of the dry season, and increased rainfall in early spring that removes these aerosols from the atmosphere through wet deposition (**Figure 10(b)**).

In summer, the contribution of dust aerosols decreases to 89.1% due to increased rainfall, which moistens the soil and limits particle suspension, as well as changes in wind direction and intensity, which reduce the transport of dust from the Sahara. Additional factors, such as increased vegetation cover due to higher humidity and a reduction in surface erosion sources, may also contribute to this decrease (**Figure 10(c)**). Sulfate aerosols contribute 10%, primarily resulting from the combustion of fossil fuels (coal and oil), which release sulfur dioxide that is subsequently converted into sulfates, and, to a lesser extent, from soil erosion prevalent during this season. Organic aerosols, originating from vegetation decomposition, biogenic emissions, biomass burning (bush and agricultural fires), motorcycle traffic, and fossil fuel combustion, contribute only 4.4%. Finally, carbonaceous aerosols (1.4%) and sea

salts (1.1%), whose contributions have increased, are largely associated with fossil fuel combustion and deforestation. Sea salts are also linked to soil salinization caused by climate change (erosion, reduced water availability) and the evaporation of saline waters. In Chad, summer conditions exacerbate these phenomena through higher temperatures and increased evaporation, enhancing the concentration of these substances in the environment, particularly the salinization of soil and surface water (Figure 10(c)).

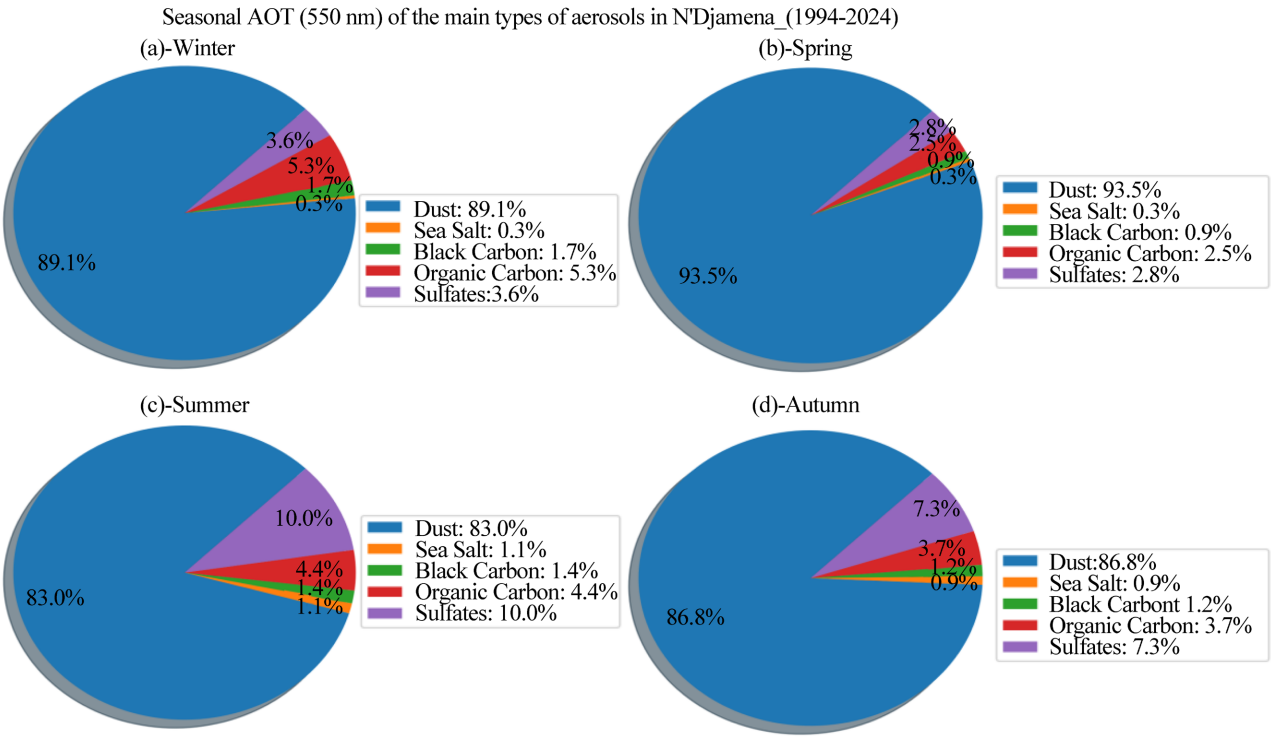

Figure 10. Percentage contributions of different types of aerosols in N'Djamena for the period 1994-2024 at MERRA-2. (a) Winter; (b) Spring; (c) Summer; (d) Fall.

With the arrival of fall, the contribution of dust aerosols decreases to 86.8%. This reduction is primarily due to the onset of monsoons and rainfall, which clean the atmosphere and stabilize the soil. The intertropical front shifts southward, slowing the transport of desert dust. In addition, Sahelian sources become less active as soils become wetter. Sulfate aerosols contribute 7.3%, a decrease explained by reduced pollution sources such as lower industrial emissions and biomass burning, more efficient atmospheric cleansing due to changes in atmospheric chemistry and precipitation, and variations in wind patterns that either transport aerosols away or promote their deposition. The contributions of organic aerosols (3.7%), carbonaceous aerosols (1.2%), and sea salts (0.9%) are mainly attributable to the reduction in dust sources and in biogenic and anthropogenic emissions. This is particularly evident at the end of the rainy season, when surface winds decrease at the beginning of the dry season and agricultural activities change. Autumn in Chad is therefore characterized by reduced wind erosion of soils and lower dust concentrations, while variations in temperature and humidity also influence natural

emissions (Figure 10(d)).

4. Conclusions

This study reveals a predominance of desert dust over Chad, largely influenced by seasonal winds, the most significant being the Harmattan and the monsoon. The intercomparison of satellite sensors with MERRA-2 also shows that MODIS (R = 0.62) is the most suitable sensor for studying aerosols in Chad, followed by MISR (R = 0.61), SeaWIFS (R = 0.55), and OMI (R = 0.41). This finding underscores the usefulness of satellite observations in compensating for the lack of ground-based instruments such as AERONET, which is absent in Chad. The MODIS sensor provides accurate data on dust concentrations. This helps refine regional climate models and better understand the impact of aerosols on precipitation patterns and local weather, which in turn influences climate forecasts. It also allows authorities to monitor better and manage air quality by identifying periods of high dust concentration, enabling environmental managers to implement emission reduction strategies and alert the public during pollution episodes, especially by formulating recommendations to reduce exposure for vulnerable individuals (children, the elderly, etc.). Moreover, it facilitates a precise understanding of dust levels to provide tailored public health advice. Lastly, the results derived from MODIS data can support scientific research and guide policy decisions regarding the management of natural resources, agriculture, and sustainable development. Additionally, the spatio-temporal analysis of aerosol indices has shown that the Chadian atmosphere is markedly dominated by absorbing aerosols in spring and autumn, such as sulfates and iron oxides, which are highly absorbent in the visible and infrared spectrum. The seasonal distribution of the Angström exponent in relation to optical thickness also indicates that the atmosphere above N'Djamena consists of a mixture of coarse-mode and accumulation-mode aerosols. This suggests that the atmosphere over Chad is made up of a mixture of aerosols from both modes (coarse mode and accumulation mode) and a scarcity of fine mode aerosols. A detailed study of the main types of atmospheric aerosols in N'Djamena has reinforced the findings of [51], which confirm the dominance of the coarse mode (primarily mineral dust) in N'Djamena. The overarching results from this study support research on the interactions between aerosols and climate, contributing to broader studies on atmospheric dynamics and their environmental impacts.

Looking ahead, this research will be extended to include aspects such as the refractive index of atmospheric aerosols, their size distribution, and their radiative balance, in order to examine their seasonal heterogeneity, their contribution according to source regions, their categorization, and their interactions with solar radiation. This will provide a better understanding of the climatic role of atmospheric aerosols over Chad.

Conflicts of Interest

The authors declare no conflicts of interest regarding the publication of this paper.

References

[1] Younous, A.A., Niang, S.A.A., Sarr, A. and Drame, M.S. (2024) Assessment of Wind Energy Resources in Chad, Central Africa, Using 100-M Wind Data from ERA5 Reanalysis. *Energy Exploration & Exploitation*, **43**, 473-491. https://doi.org/10.1177/01445987241302424

[2] Engelstaedter, S., Tegen, I. and Washington, R. (2006) North African Dust Emissions and Transport. *Earth-Science Reviews*, **79**, 73-100. https://doi.org/10.1016/j.earscirev.2006.06.004

[3] Guirado, C., Cuevas, E., Cachorro, V.E., Toledano, C., Alonso-Pérez, S., Bustos, J.J., *et al.* (2014) Aerosol Characterization at the Saharan AERONET Site Tamanrasset. *Atmospheric Chemistry and Physics*, **14**, 11753-11773. https://doi.org/10.5194/acp-14-11753-2014

[4] Bristow, C.S., Drake, N. and Armitage, S. (2009) Deflation in the Dustiest Place on Earth: The Bodélé Depression, Chad. *Geomorphology*, **105**, 50-58. https://doi.org/10.1016/j.geomorph.2007.12.014

[5] Ben-Ami, Y., Koren, I., Rudich, Y., Artaxo, P., Martin, S.T. and Andreae, M.O. (2010) Transport of North African Dust from the Bodélé Depression to the Amazon Basin: A Case Study. *Atmospheric Chemistry and Physics*, **10**, 7533-7544. https://doi.org/10.5194/acp-10-7533-2010

[6] Ernest, A., Laryea, N., Oluwaseun, O.O., Kofi, A.S., Oduro, N.B., *et al.* (2022) Dust Sources and Impact: A Review. *North American Academic Research*, **5**, 17-37.

[7] Nébon, B., Dramé, M.S., Sall, S.M., Bruno, K., Niang, D.N., Florent, K.P., *et al.* (2019) Intra-Seasonal and Annual Variation of Aerosols and Their Radiative Impact in the Sahelian Zone of Burkina Faso. *Atmospheric and Climate Sciences*, **9**, 62-74. https://doi.org/10.4236/acs.2019.91004

[8] Orozi, G., Tchiroue, K. and Halawlaw, Y.I. (2022) Analysis of Natural Aerosols' Vertical Distribution in Sahelian Zone via the OPEN (Clouds Seeding Operation) Project in Chad. *International Journal of Current Research and Academic Review*, **10**, 7-17.

[9] Liu, Y., Huang, J. and Huang, F. (2023) A Comprehensive Review on Study Methods of Aerosol Optical Properties in Different Dimensions. *IEEE Access*, **11**, 36763-36786. https://doi.org/10.1109/access.2023.3266333

[10] Diarra, C. and Ba, A. (2014) Analyse des paramètres optiques des aérosols atmosphériques, de leur distribution et de leur albédo de diffusion par les mesures photométriques au Mali. *Afrique Science*, **10**, 82-97.

[11] Diarra, C., Coulibaly, A.H. and Sow, M. (2019) Caracterisation de types d'aerosols atmospheriques par l'analyse de donnees photometriques du reseau aeronet en afrique de l'ouest.

[12] (2015) Changements climatiques 2014: Rapport de synthèse: Contribution des Groupes de travail I, II et III au cinquième Rapport d'évaluation du Groupe d'experts intergouvernemental sur l'évolution du climat. GIEC.

[13] Mulago, S.K., Makokha, J.W. and Boiyo, R. (2024) Spatial-Temporal Variation of Aerosol Optical Depth and Ångström Exponent over Selected Towns in Kenya: Environmental Impact and Climate Change. *OALib*, **11**, 1-16. https://doi.org/10.4236/oalib.1111803

[14] Goni, S., Adannou, H.A., Diop, D., Kriga, A., Khayal, A.Y., Nebon, B., *et al.* (2019) Observation and Simulation of Available Solar Energy at N'djamena, Chad. *Smart Grid and Renewable Energy*, **10**, 165-178. https://doi.org/10.4236/sgre.2019.106011

[15] Marticorena, B., Haywood, J., Coe, H., Formenti, P., Liousse, C., Mallet, M., *et al.*

(2011) Tropospheric Aerosols over West Africa: Highlights from the AMMA International Program. *Atmospheric Science Letters*, **12**, 19-23. https://doi.org/10.1002/asl.322

[16] Schwanghart, W. and Schütt, B. (2008) Meteorological Causes of Harmattan Dust in West Africa. *Geomorphology*, **95**, 412-428. https://doi.org/10.1016/j.geomorph.2007.07.002

[17] Washington, R. and Todd, M.C. (2005) Atmospheric Controls on Mineral Dust Emission from the Bodélé Depression, Chad: The Role of the Low Level Jet. *Geophysical Research Letters*, **32**, e2005GL023597. https://doi.org/10.1029/2005gl023597

[18] Korgo, B. (2014) Caractérisation optique et microphysique des aérosols atmosphériques en zone urbaine ouest africaine: Application aux calculs du forçage radiatif à Ouagadougou. Master's Thesis, Universite de Ouagadougou.

[19] Yusuf, N., Said S, R., Tilmes, S. and Gbobaniyi, E. (2021) Multi-Year Analysis of Aerosol Optical Properties at Various Timescales Using AERONET Data in Tropical West Africa. *Journal of Aerosol Science*, **151**, Article ID: 105625. https://doi.org/10.1016/j.jaerosci.2020.105625

[20] Pierangelo, C. (2005) Apports du sondage infrarouge à l'étude des aérosols atmosphériques. Master's Thesis, Université Pierre et Marie Curie—Paris VI.

[21] Bado, N., Bazyomo, S.D., Ouedraogo, G.W.P., Korgo, B., Dramé, M.S., Kieno, F.P., *et al.* (2024) Contribution of Satellite Observations in the Optical and Microphysical Characterization of Aerosols in Burkina Faso, West Africa. *Atmospheric and Climate Sciences*, **14**, 154-171. https://doi.org/10.4236/acs.2024.141010

[22] Bedoum, A., Biona, C.B. and Adoum, I. (2014) Impact de la variabilité pluviométrique et de la sécheresse au sud du tchad: Effets du changement climatique. *Revue Ivoirienne des Sciences et Technologie*, **23**, 13-30.

[23] Remini, B. (2018) Tibesti-Ennedi-Chad Lake: The Triangle of Dust Impact on the Fertilization of the Amazonian Forest. *Larhyss Journal*, No. 34, 147-182.

[24] Senghor, H., Machu, É., Hourdin, F. and Gaye, A.T. (2017) Seasonal Cycle of Desert Aerosols in Western Africa: Analysis of the Coastal Transition with Passive and Active Sensors. *Atmospheric Chemistry and Physics*, **17**, 8395-8410. https://doi.org/10.5194/acp-17-8395-2017

[25] Bado, N., Ouédraogo, A., Guengané, H., Maurice Ky, T.S., Bazyomo, S.D., Korgo, B., *et al.* (2019) Climatological Analysis of Aerosols Optical Properties by Airborne Sensors and *in Situ* Measurements in West Africa: Case of the Sahelian Zone. *Open Journal of Air Pollution*, **8**, 118-135. https://doi.org/10.4236/ojap.2019.84007

[26] Filonchyk, M. and Hurynovich, V. (2020) Validation of MODIS Aerosol Products with AERONET Measurements of Different Land Cover Types in Areas over Eastern Europe and China. *Journal of Geovisualization and Spatial Analysis*, **4**, Article No. 10. https://doi.org/10.1007/s41651-020-00052-9

[27] Mhawish, A., Banerjee, T., Sorek-Hamer, M., Lyapustin, A., Broday, D.M. and Chatfield, R. (2019) Comparison and Evaluation of MODIS Multi-Angle Implementation of Atmospheric Correction (MAIAC) Aerosol Product over South Asia. *Remote Sensing of Environment*, **224**, 12-28. https://doi.org/10.1016/j.rse.2019.01.033

[28] Peyridieu, S., *et al.* (2010) Saharan Dust Infrared Optical Depth and Altitude Retrieved from AIRS: A Focus over North Atlantic—Comparison to MODIS and CALIPSO. *Atmospheric Chemistry and Physics*, **10**, 1953-1967.

[29] Bibi, H., Alam, K., Chishtie, F., Bibi, S., Shahid, I. and Blaschke, T. (2015) Intercomparison of MODIS, MISR, OMI, and CALIPSO Aerosol Optical Depth Retrievals for Four Locations on the Indo-Gangetic Plains and Validation against AERONET Data.

Atmospheric Environment, **111**, 113-126.
https://doi.org/10.1016/j.atmosenv.2015.04.013

[30] Cuevas, E., Camino, C., Benedetti, A., Basart, S., Terradellas, E., Baldasano, J.M., *et al.* (2015) The MACC-II 2007-2008 Reanalysis: Atmospheric Dust Evaluation and Characterization over Northern Africa and the Middle East. *Atmospheric Chemistry and Physics*, **15**, 3991-4024. https://doi.org/10.5194/acp-15-3991-2015

[31] Prospero, J.M., Ginoux, P., Torres, O., Nicholson, S.E. and Gill, T.E. (2002) Environmental Characterization of Global Sources of Atmospheric Soil Dust Identified with the Nimbus 7 Total Ozone Mapping Spectrometer (TOMs) Absorbing Aerosol Product. *Reviews of Geophysics*, **40**, 2-1-2-31. https://doi.org/10.1029/2000rg000095

[32] Washington, R., Todd, M., Middleton, N.J. and Goudie, A.S. (2003) Dust-Storm Source Areas Determined by the Total Ozone Monitoring Spectrometer and Surface Observations. *Annals of the Association of American Geographers*, **93**, 297-313. https://doi.org/10.1111/1467-8306.9302003

[33] Bounhir, A., Benkhaldoun, Z. and Sarazin, M. (2007) Aerosol Characterization of Morocco with AERONET and Intercomparison with Satellite Data: TOMS, MODIS and Misr. *SPIE Proceedings*, **6745**, Article ID: 674506.
https://doi.org/10.1117/12.730818

[34] Krueger, A.J., Walter, L.S., Bhartia, P.K., Schnetzler, C.C., Krotkov, N.A., Sprod, I., *et al.* (1995) Volcanic Sulfur Dioxide Measurements from the Total Ozone Mapping Spectrometer Instruments. *Journal of Geophysical Research*: *Atmospheres*, **100**, 14057-14076. https://doi.org/10.1029/95jd01222

[35] Al-Salihi, A.M. (2018) Characterization of Aerosol Type Based on Aerosol Optical Properties over Baghdad, Iraq. *Arabian Journal of Geosciences*, **11**, Article No. 633.
https://doi.org/10.1007/s12517-018-3944-1

[36] Raptis, I., Kazadzis, S., Amiridis, V., Gkikas, A., Gerasopoulos, E. and Mihalopoulos, N. (2020) A Decade of Aerosol Optical Properties Measurements over Athens, Greece. *Atmosphere*, **11**, Article 154. https://doi.org/10.3390/atmos11020154

[37] Chaabane, M., Elleuch, F., Masmoudi, M. and Medhioub, K. (2007) Caractérisation d'un photomètre solaire conçu pour l'étude des propriétés optiques des aérosols atmosphériques. 18*è Congrès Français de Mécanique*, Grenoble, 27-31 August 2007, 1-6.

[38] Korgo, B., Roger, J.-C. and Bathiebo, J. (2013) Climatology of Air Mass Trajectories and Aerosol Optical Thickness over Ouagadougou. *Global Journal of Pure and Applied Sciences*, **19**, 169-181.

[39] Basart, S., Perez, C., Cuevas, E., Baldasano, J.M. and Gobbi, G.P. (2009) Aerosol Characterization in Northern Africa, Northeastern Atlantic, Mediterranean Basin and Middle East from Direct-Sun AERONET Observations. *Atmospheric Chemistry and Physics*, **9**, 8265-8282.

[40] Filonchyk, M., Hurynovich, V., Yan, H., Zhou, L. and Gusev, A. (2019) Climatology of Aerosol Optical Depth over Eastern Europe Based on 19 Years (2000-2018) MODIS TERRA Data. *International Journal of Climatology*, **40**, 3531-3549.
https://doi.org/10.1002/joc.6412

[41] Ichoku, C., Chu, D.A., Mattoo, S., Kaufman, Y.J., Remer, L.A., Tanré, D., *et al.* (2002) A Spatio-Temporal Approach for Global Validation and Analysis of MODIS Aerosol Products. *Geophysical Research Letters*, **29**, MOD1-1-MOD1-4.
https://doi.org/10.1029/2001gl013206

[42] Tripathi, S.N., Dey, S., Chandel, A., Srivastava, S., Singh, R.P. and Holben, B.N. (2005) Comparison of MODIS and AERONET Derived Aerosol Optical Depth over the Ganga Basin, India. *Annales Geophysicae*, **23**, 1093-1101.

https://doi.org/10.5194/angeo-23-1093-2005

[43] Hyer, E.J., Reid, J.S. and Zhang, J. (2011) An Over-Land Aerosol Optical Depth Data Set for Data Assimilation by Filtering, Correction, and Aggregation of MODIS Collection 5 Optical Depth Retrievals. *Atmospheric Measurement Techniques*, **4**, 379-408. https://doi.org/10.5194/amt-4-379-2011

[44] Misra, A., Tripathi, S.N., Kaul, D.S. and Welton, E.J. (2012) Study of MPLNET-Derived Aerosol Climatology over Kanpur, India, and Validation of CALIPSO Level 2 Version 3 Backscatter and Extinction Products. *Journal of Atmospheric and Oceanic Technology*, **29**, 1285-1294. https://doi.org/10.1175/jtech-d-11-00162.1

[45] Awoleye, P.O., Ogunjobi, K.O. and Balogun, I.A. (2024) Climatology and Dynamics of Aerosol Optical Properties from Selected AERONET Sites over West Africa. *Discover Atmosphere*, **3**, Article No. 11.

[46] Chiapello, I. and Moulin, C. (2002) TOMS and METEOSAT Satellite Records of the Variability of Saharan Dust Transport over the Atlantic during the Last Two Decades (1979-1997). *Geophysical Research Letters*, **29**, 17-1-17-4. https://doi.org/10.1029/2001gl013767

[47] Formenti, P., Schütz, L., Balkanski, Y., Desboeufs, K., Ebert, M., Kandler, K., *et al.* (2011) Recent Progress in Understanding Physical and Chemical Properties of African and Asian Mineral Dust. *Atmospheric Chemistry and Physics*, **11**, 8231-8256. https://doi.org/10.5194/acp-11-8231-2011

[48] Andreae, M.O. (2019) Emission of Trace Gases and Aerosols from Biomass Burning—An Updated Assessment. *Atmospheric Chemistry and Physics*, **19**, 8523-8546. https://doi.org/10.5194/acp-19-8523-2019

[49] Bond, T.C., Doherty, S.J., Fahey, D.W., Forster, P.M., Berntsen, T., DeAngelo, B.J., *et al.* (2013) Bounding the Role of Black Carbon in the Climate System: A Scientific Assessment. *Journal of Geophysical Research*: *Atmospheres*, **118**, 5380-5552. https://doi.org/10.1002/jgrd.50171

[50] Liousse, C., Guillaume, B., Grégoire, J.M., Mallet, M., Galy, C., Pont, V., *et al.* (2010) Updated African Biomass Burning Emission Inventories in the Framework of the AMMA-IDAF Program, with an Evaluation of Combustion Aerosols. *Atmospheric Chemistry and Physics*, **10**, 9631-9646. https://doi.org/10.5194/acp-10-9631-2010

[51] Tobias, C. and Megie, C. (1980) Les lithométéores au Tchad: Premiers résultats concernant la nature, la composition et l'importance des aérosols transportés par voie atmosphérique dans la région de N'Djamena (Tchad). *Cahiers ORSTOM Série Pédologie*, **18**, 71-81.

[52] Carmona, I. and Alpert, P. (2009) Synoptic Classification of Moderate Resolution Imaging Spectroradiometer Aerosols over Israel. *Journal of Geophysical Research*: *Atmospheres*, **114**, e2008JD010160. https://doi.org/10.1029/2008jd010160